NUREG/CR-4615
LA-10730-MS
Vol. 2

Modeling Study of Solute Transport in the Unsaturated Zone

NUREG/CR--4615-Vol.2

TI87 009181

Workshop Proceedings

Manuscript Completed: February 1987
Date Published: April 1987

Edited by
E. P. Springer, H. R. Fuentes*

T. Mo, NRC Project Manager

Los Alamos National Laboratory
Los Alamos, NM 87545

*Department of Civil Engineering, University of Texas-El Paso, El Paso, TX 79968

Prepared for
Division of Waste Management
Office of Nuclear Material Safety and Safeguards
U.S. Nuclear Regulatory Commission
Washington, DC 20555
NRC FIN A7150

DISCLAIMER

ANALYSIS AND PREDICTION OF WATER AND SOLUTE TRANSPORT IN A LARGE LYSIMETER

M. Th. van Genuchten,[1]
J. C. Parker,[2] and J. B. Kool[2]
[1]U.S. Salinity Laboratory
4500 Glenwood Drive
Riverside, California 92501
[2]Department of Agronomy
Virginia Polytechnic Institute
and State University
Blacksburg, Virginia 24061

INTRODUCTION

Our purpose in this report is to undertake the deterministic description of properties governing water and solute transport for crushed Bandelier Tuff in lysimeter experiments carried out at Los Alamos National Laboratory, New Mexico. Specifically, we will consider experiments performed on compacted crushed tuff in caissons A and B of the experimental cluster described by DePoorter (1981). Our principal objective is to analyze the results of bromide (Br), iodide (I), lithium (Li), and strontium (Sr) tracer experiments performed in caisson B under near-steady flow conditions using selected analytical and numerical solutions of the classical deterministic convection-dispersion equation for steady flow in an assumed uniform velocity field. Although in the present analyses of transport we will treat the flow problem in a simplistic fashion, other studies currently being conducted parallel to this one, as well as anticipated future studies, will require a more rigorous treatment of the hydrologic behavior. Therefore, in addition to the analyses of the caisson B transport experiments, we have undertaken a number of analyses to characterize the hydraulic behavior of crushed Bandelier Tuff from water content and pressure head measurements obtained during transient drainage experiments on material in caisson A and, for some analyses, also employed selected laboratory data.

MODEL DESCRIPTION

Hydraulic Properties

Soil water retention and hydraulic conductivity functions are assumed to be represented by the model of van Genuchten (1980) as

$$\theta = \theta_r + \frac{\theta_s - \theta_r}{(1+|\alpha h|^n)^m} \tag{1}$$

and

$$K = K_s S_e^{\ell} [1 - (1 - S_e^{1/m})^m]^2, \tag{2}$$

where θ is the volumetric water content; θ_r and θ_s are residual and field-saturated water contents, h is the pressure head; α, ℓ, and n are empirical shape factors: m = 1-1/n; K_s is the field-saturated hydraulic conductivity; and S_e is effective fluid saturation defined by

$$S_e = \frac{\theta - \theta_r}{\theta_s - \theta_r}. \tag{3}$$

Various methods of estimating the parameters K_s, θ_s, θ_r, α, n, and ℓ to describe the hydraulic properties of crushed Bandelier Tuff used in the caisson tracer experiments will be considered subsequently.

Transport Studies

Solute transport during steady state flow is described in this study by the one-dimensional deterministic convection-dispersion equation

$$\frac{\partial C}{\partial t} + \frac{\rho}{\theta}\frac{\partial s}{\partial t} = D\frac{\partial^2 C}{\partial x^2} - v\frac{\partial C}{\partial x}, \tag{4}$$

where C is the solute concentration, s is the adsorbed concentration, D is the dispersion coefficient, ρ is the bulk density, θ is the water content, $v = q/\theta$ is the pore water velocity where q is the hydraulic flux density, x is distance, and t is time. Equilibrium adsorbed and solute concentrations are related by a Freundlich-type isotherm of the form

$$s = kC^{\eta}, \tag{5}$$

where k and η are empirical parameters. Assuming local equilibrium conditions exist, substitution of (5) into (4) yields

$$R\frac{\partial C}{\partial t} = D\frac{\partial^2 C}{\partial x^2} - v\frac{\partial C}{\partial x}, \tag{6}$$

in which the nonlinear retardation factor R is given by

$$R = 1 + \rho k\eta C^{\eta-1}/\theta. \tag{7}$$

For linear adsorption, $\eta = 1$ and R becomes independent of concentration:

$$R = 1 + \rho k/\theta. \tag{8}$$

The parameter k in (8) is often referred to as the distribution coefficient K_d.

Equation (6) is solved subject to a uniform initial concentration C_i and a pulse-type boundary condition at the soil surface:

$$\left(-D \frac{\partial C}{\partial x} + vC\right) \Big|_{x=0} = \begin{cases} vC_o & 0 \leq t < t_o \\ 0 & t \geq t_o \end{cases} , \qquad (9)$$

where C_o is the input concentration and t_o is the solute pulse duration. Assuming a semi-infinite profile ($0 \leq x < \infty$), linear adsorption ($\eta = 1$), and solute detection in flux concentration mode [$c_f = c-(D/v)\ \partial c/\partial x$; see Parker and van Genuchten 1984a], the appropriate analytical solution to (6) subject to (9) is

$$C_f(x,t) = \begin{cases} C_o\ A(x,t) & 0 \leq t < t_o \\ C_o\ A(x,t) - C_o\ A(x,t-t_o) & t \geq t_o \end{cases} , \qquad (10a)$$

where

$$A(x,t) = \frac{1}{2} \operatorname{erfc}\left[\frac{Rx - vt}{2(DRt)^{1/2}}\right] + \frac{1}{2} \exp\left[\frac{vx}{D}\right] \operatorname{erfc}\left[\frac{Rx + vt}{2(DRt)^{1/2}}\right] . \qquad (10b)$$

Equation (10) assumes that observed concentrations represent flux-averaged concentrations rather than volume-averaged resident concentrations. Observed concentrations determined in suction samplers may correspond precisely to neither flux nor resident concentrations; however, because of the generally small values of the dimensionless groups (vx/D) obtained in this study, differences between the two concentration modes should be extremely small (Parker and van Genuchten 1984a) so the distinction need not be of concern.

For cases of nonlinear adsorption, we solve (6) with an iterative numerical method based on a Crank-Nicolson-type finite difference formulation of the governing equations.

METHODS OF ANALYSIS

Hydraulic Properties

Two parameter estimation methods employing different objective functions and input data were used to quantify the parameters in the hydraulic model described by Equations (1) and (2) for crushed Bandelier Tuff. In Method 1, K_s, θ_r, α, and n are estimated from water content and pressure head observations in caisson A during a transient drainage experiment (Abeele 1984). The average water content after ponding for more than one month provided an independent estimate for θ_s of 0.331. From Mualem (1976), the coefficient ℓ in Equation (2) was assumed to be 0.5, thus leaving four unknown coefficients including the saturated conductivity. Abeele (1984) estimated the latter to be about 12.4 cm/d from the steady state lysimeter drainage rate: however, owing to uncertainty in the parametric model near the transition from saturated to unsaturated conditions as well as to experimental uncertainties, we regard K_s to be an unknown in the present analysis.

The unknown parameters were estimated from measured water contents at 6 depths (0.4, 1.16, 1.91, 2.71, 3.47, and 4.23 m) and measured pressure heads at only one depth (0.4 m) observed over a period of 100 days as the caisson drained from saturation subject to a zero surface flux. The inverse problem was solved by combining a numerical solution of the one-dimensional unsaturated flow equation with a nonlinear least-squares optimization scheme based on the Levenberg-Marquardt method (Marquardt 1963). The unsaturated flow equation was taken as

$$C(h)\ \frac{\partial h}{\partial t} = \frac{\partial}{\partial x}\ [K(h)\ \frac{\partial h}{\partial x} - K(h)], \qquad (11)$$

where $C(h) = d\theta/dh$ is the soil water capacity, x is depth from the soil surface, and t is time.

The optimization program used in this study is a modification of the code of Kool et al. (1985). In this model, Equation (11) is solved with a fully implicit, Galerkin-type, mass-lumped linear finite element scheme. This scheme has proved to be considerably more efficient than the previously employed Hermitian cubic scheme. The objective function O(b) to be minimized was taken to be of the form

$$O(b) = \sum_{i=1}^{m} \sum_{j=1}^{p} [\theta_{ij}^{*} - \theta_{ij}(b)]^2 + \sum_{j=1}^{p} W[h_j^{*} - h_j(b)]^2, \quad (12)$$

where θ_{ij}^{*} represents measured water contents at m = 5 depths x_i and p = 6 times t_j: h_j^{*} is the measured pressure head at x = 0.4 m and times t_j: and $\theta_{ij}(b)$ and $h_j(b)$ are model-predicted θ and h corresponding to parameter vector $b = (\alpha, \theta_r, n, K_s)$. The weighting coefficient W was chosen such that the two composite terms of (12) attain roughly the same value (Parker et al. 1985).

The unknown parameters in Equations (1) and (2) were also estimated directly (Method 2) from the reported $\theta(h)$ and K(h) data listed in Table III of Abeele (1984). To obtain better resolution at relatively low water contents, we augmented the caisson data with laboratory-measured data for h $\lesssim$ -300 cm from an earlier study by Abeele (1979). The objective function in Method 2 was taken to be

$$O(b) = \sum_{i=1}^{M} [\theta_i^{*} - \theta_i(b)]^2 + \sum_{j=1}^{N} V[\log(K_j^{*}) - \log(K_j(b))]^2, \quad (13)$$

where θ_i^* and $\theta_i(b)$ are observed and predicted water contents at M pressure heads, K_j^* and $K_j(b)$ are observed and predicted conductivities at N heads, and V is a weighting factor that ensures roughly equal values of the two terms of (13). Two different analyses with Method 2 were performed with different unknown parameter vectors b. In Method 2a all six parameters (θ_r, θ_s, α, n, ℓ, K_s) were treated as unknown, while in Method 2b θ_s and K_s were fixed at their measured values and only θ_r, α, n, and ℓ were estimated.

Transport Studies

Observed concentration data in caisson B were analyzed using the CXTFIT program of Parker and van Genuchten (1984b). Subject to a few restrictions, this program can be used to optimize the unknown coefficients v, D, R, and t_o in Equations (6) and (9) from observed temporal and spatial concentration data. One restriction is that v and R cannot be optimized simultaneously because of similar effects on the effective transport rate v/R in the soil column. We assumed that iodide and bromide were not adsorbed on, nor excluded from, the solid phase, resulting in R=1. Table 1 lists all measured or independently estimated parameter values and indicates those parameters that were treated as unknowns in the parameter estimation process. For the iodide and bromide displacement experiments, the parameters v, D, and t_o were treated as unknowns, whereas R was taken to be unity with no adsorption. Similarly, the parameters D, R, and t_o were considered unknowns for the lithium tracer experiments, while v was fixed at 11.7 cm/d as estimated from the iodide and bromide data (to be discussed later). To simulate strontium transport, nonlinearity in the adsorption behavior was explicitly considered. From Polzer et al. (1985), the Freundlich exponent η for Sr was taken to be 0.835. Values for v and D

were assumed to be the same as those in the iodide and bromide experiments. Since independent estimates for θ, ρ, and t_o were also available, the only unknown parameter that remained to be estimated from the tracer experiments was the Freudlich k-value in Equation (5), which was obtained by matching observed and predicted concentrations during initial breakthrough.

Table 1. Assumed unknown parameters (indicated by "?") and measured data (indicated by value) for the iodide, bromide, lithium, and strontium tracer experiments.

Parameter	Iodide	Bromide	Lithium	Strontium
θ (cm^3/cm^3)	-[a]	-	0.28	0.28
ρ (g/cm^3)	-	-	1.60	1.60
C_i (mg/L)	0.2	0.0	0.04	0.2
C_o (mg/L)	170.0	79.0	6.80	70.0
v (cm/d)	?	?	11.70[b]	11.70[b]
D (cm^2/d)	?	?	?	4.72[c]
t_o (days)	?	?	?	6.0
R	1.0	1.0	?	?
k ($\mu g^{1-\eta} cm^{3\eta} g^{-1}$)	-	-	-	?
η	-	-	1.0	0.835

[a] Not needed in estimation process.

[b] Estimated from iodide and bromide experiments.

[c] Estimated from iodide, bromide, and lithium experiments.

RESULTS AND DISCUSSION

Hydraulic Properties

Values for parameters in the soil hydraulic functions [Equations (1) and (2)] estimated by Methods 1, 2a, and 2b are given in Table 2. Figure 1 compares the fitted retention and hydraulic conductivity curves of Method 2a with the laboratory and caisson-derived data of Abeele (1979, 1984). The estimated curves for Method 1 are not shown on the figure but nearly duplicate the calculated curves for Method 2a, even though some of the parameter values for Method 1 were quite different (notably ℓ). Small deviations occurred at lower water contents because of the difference in estimated θ_r values (Table 2) and at the higher water contents because of somewhat different K_s estimates. Note the relatively wide 95% confidence limits on K_s in Table 2 for both methods, indicating poor identifiability of K_s.

Figure 2 compares observed water content distributions in the caisson after 1, 4, 20, and 100 days (Abeele 1984) with the predicted curves using parameter estimates from Method 1 (dashed lines) and Method 2a (solid lines). Predictions were obtained by assuming that the tuff and underlying sand layer had the same hydraulic properties. The bottom boundary of the sand layer at the interface with the underlying gravel was maintained at saturation (h=0), while a no-flux condition was imposed at the soil surface. Note that the observed data are underpredicted after 1 day of drainage but are predicted very well at all other times, with Method 1 parameters generating somewhat higher water contents than those obtained with Method 2a parameters. Deviations between computed and observed distributions at 1 day are likely due to the high estimated K_s values. Abeele (1984) estimated K_s to be only about 12.4 cm/d, which would result

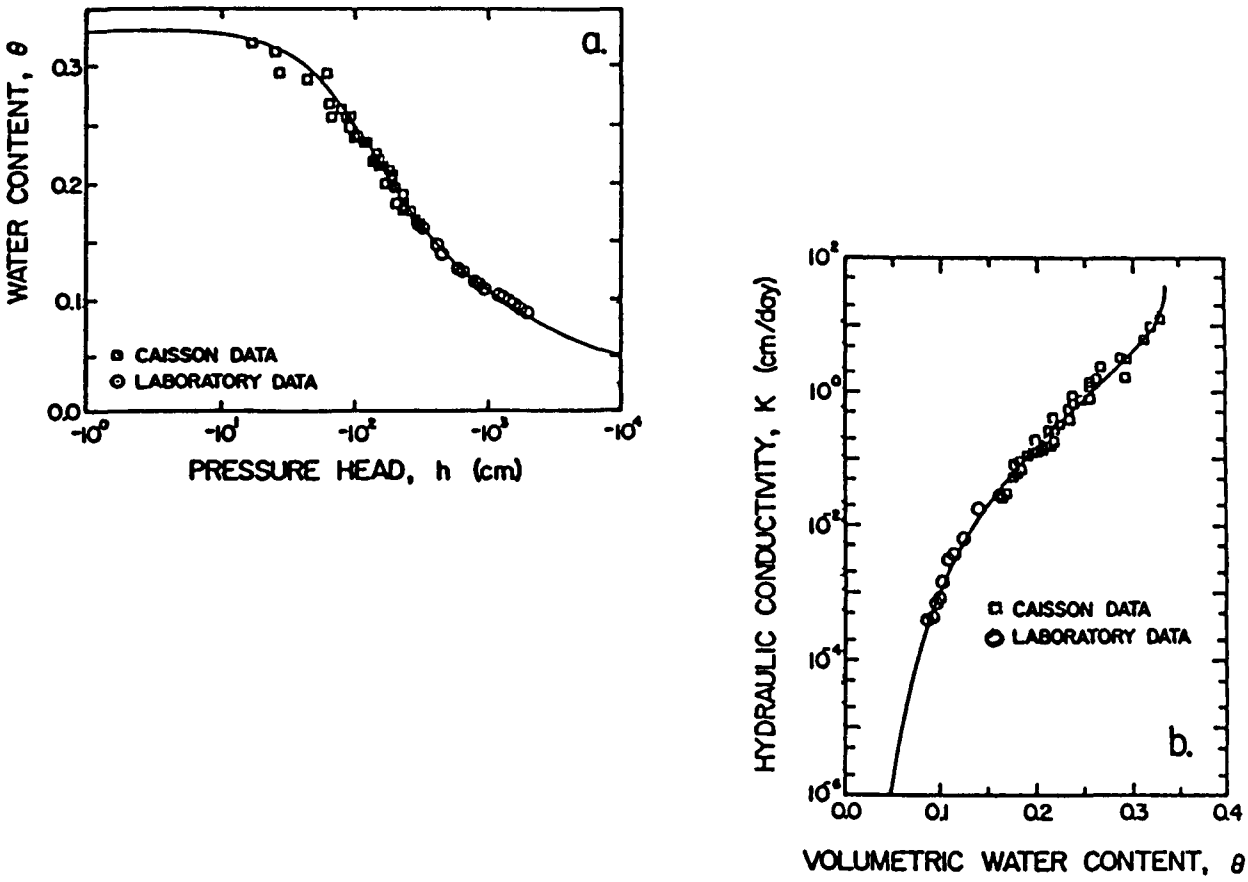

Figure 1. Measured hydraulic properties of crushed Bandelier Tuff (data points) and model-predicted properties using Method 2a parameter estimates (smooth curves).

in high predicted water contents at one day. This is shown in Figure 3 where predicted water contents using Method 2b hydraulic parameters are compared with the observed data. While predicted water contents at 1 day in this case are larger than those shown in Figure 2, drainage at later times proceeds too slowly and causes the water contents to remain high, notably at intermediate times. We conclude that the Method 1 or 2a parameters are the preferred ones for most calculations, except for near-saturated conditions.

Table 2. Parameters in Equations (1) and (2) for Bandelier Tuff estimated from in situ drainage data (Method 1) and from previously measured hydraulic data (Method 2).

Parameter	Method 1	Method 2a	Method 2b
θ_r	0.01[a]	0.0255 (±0.0185)[b]	0.0451 (±0.0066)
θ_s	0.3308[c]	0.3320 (±0.0059)	0.3308[c]
α (cm^{-1})	0.01433 (±0.0030)	0.01545 (±0.0022)	0.01339 (±0.0090)
n	1.506 (±0.105)	1.474 (±0.744)	1.636 (±0.0438)
ℓ	0.5[c]	0.4946 (±0.3713)	-1.129 (±0.2575)
K_s (cm/d)	25.0 (±12.6)	33.71 (±16.92)	12.4[c]

[a] Converging towards negative value; set to zero during estimation process.

[b] Values in parentheses indicate 95% confidence limits.

[c] Assumed to be known.

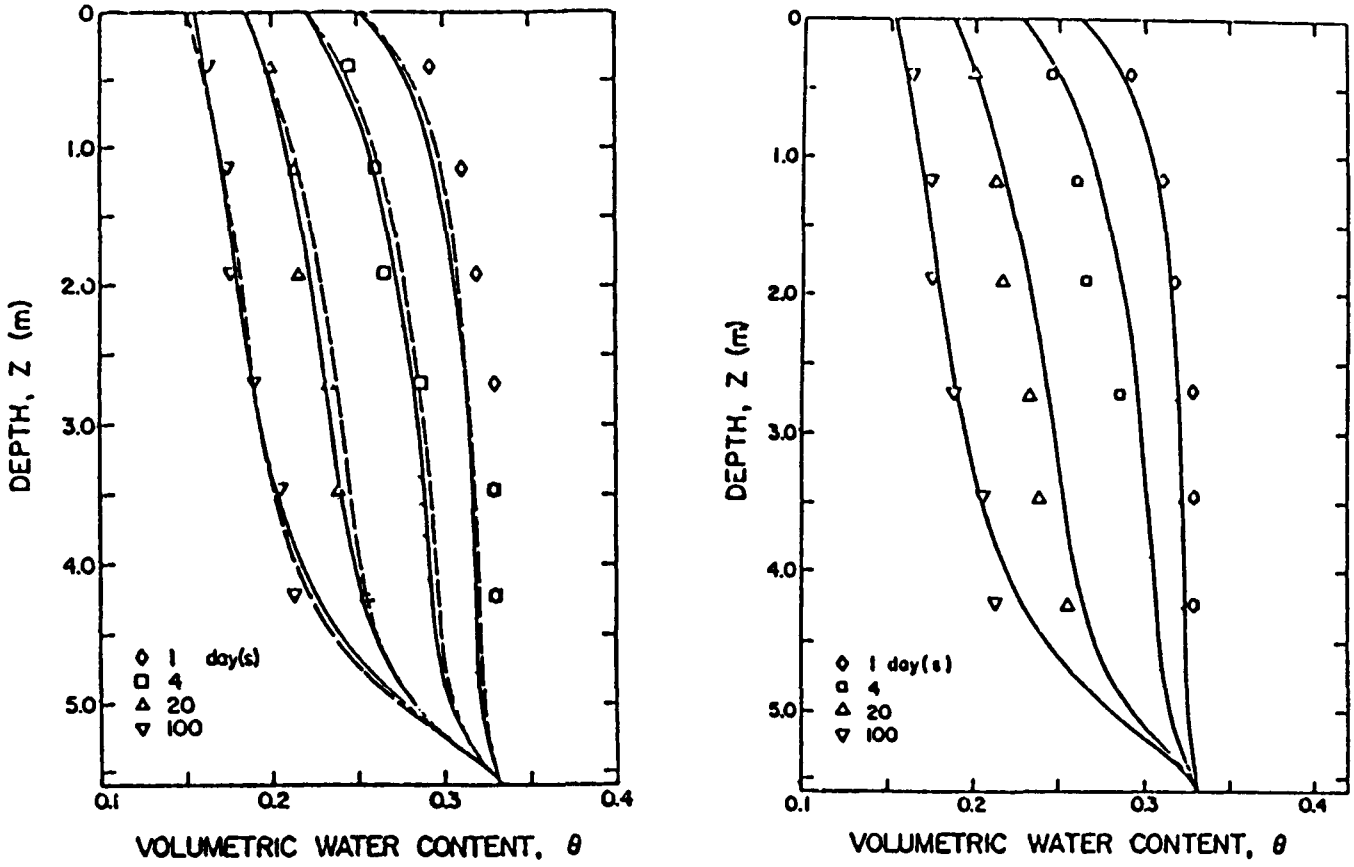

Figure 2. Measured water content profiles at different times during transient drainage under zero-flux surface condition in caisson A (data points) and predicted distributions using Method 1 parameters (a, dashed lines), Method 2a parameters (a, solid lines), and Method 2b parameters (b, solid lines).

Transport Studies

Observed tracer breakthrough curves obtained with hollow fiber suction samplers at six depths are shown in Figures 3 and 4 for bromide and iodide, respectively. All data considered here are for the tracer pulses begun on December 6, 1984, under approximately steady flow conditions. Each depth was first analyzed individually to find optimal values for v, D, and t_o assuming R = 1; these results are summarized in Table 3. For both tracers the first depth shows a relatively large D-value, probably as a consequence of the uneven application of water and tracers at the soil surface through multiple point sources. Values of v and D at this depth are relatively poorly defined as reflected by large 95% confidence intervals. As the tracers move downwards, the estimated parameters, in particular the pore water velocity, become better defined. The fitted value for t_o is in most cases significantly less than the target value of six days. Because of this discrepancy, we elected to keep t_o as an unknown parameter in this study. Note also that the peak concentrations of the 36- and 113-cm-depth observed bromide breakthrough curves are much higher than the input concentration C_o. Too few input concentration measurements were carried out during the six day pulse application to verify the accuracy of C_o. Since we are assuming C_o is known, any error in this value will effectively be accommodated by adjusting t_o to obtain apparent mass balance.

The data in Table 3 also reveal much higher fitted v-values for iodide and bromide at the 264-cm-depth port compared with the other depths. Vertical variations in the pore water velocity, due for example to differences in compaction, might be suggested as a possible explanation of this behavior. If the average pore water velocity between 0 and 188 cm is taken to be about 12.6 cm/d (see the 188-cm data in Table 3), then an

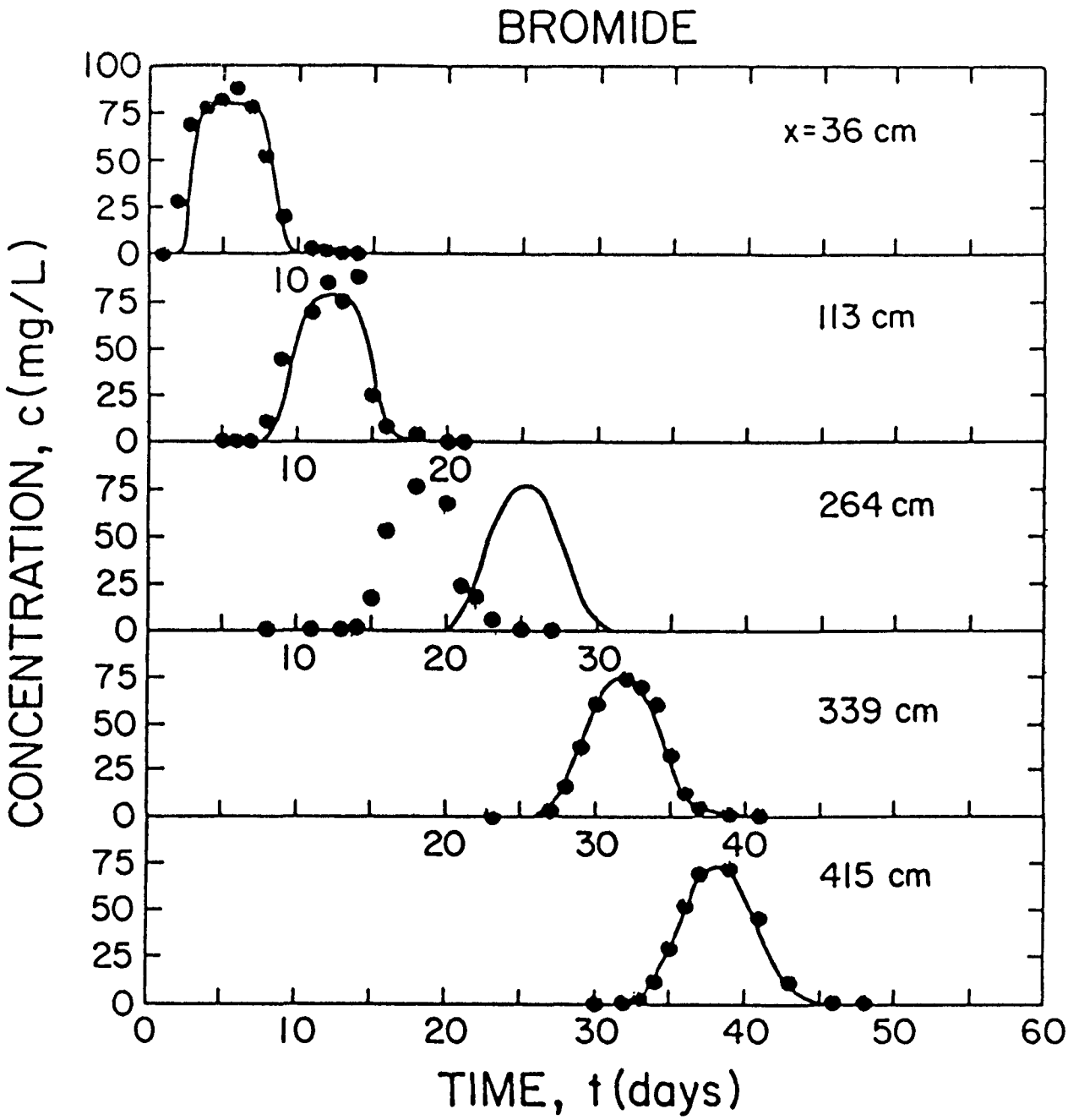

Figure 3. Bromide breakthrough curves measured at various depths in hollow fiber samplers and predicted curves using parameter values estimated from pooled iodide, bromide, and lithium data.

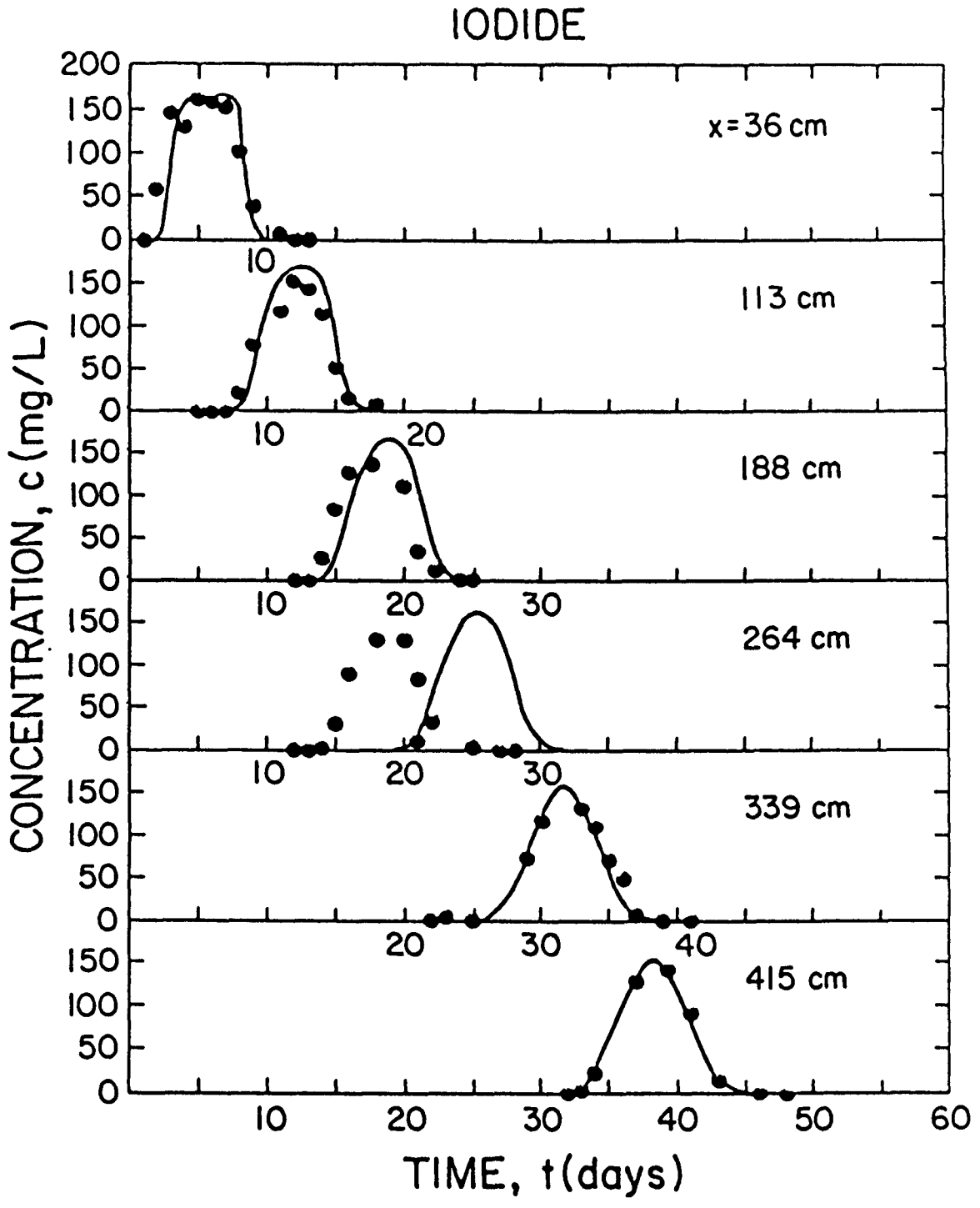

Figure 4. Iodide breakthrough curves measured at various depths in hollow fiber samplers and predicted curves using parameter values estimated from pooled iodide, bromide, and lithium data.

Table 3. Estimated values for the pore water velocity v, the dispersion coefficient D, and the pulse time t_o, for the iodide and bromide experiment in caisson B, assuming R=1 for both tracers.

Depth (cm)	v (cm/d)	D cm^2/d)	t_o (day)
	IODIDE		
36	14.45 (±1.33)[a]	53.07 (±28.37)	5.93 (±0.31)
113	11.88 (±0.36)	15.93 (± 5.07)	5.06 (±0.36)
188	12.44 (±0.15)	6.87 (± 2.53)	5.23 (±0.27)
188[b]	12.80 (±0.14)	11.06 (± 2.62)	4.98 (±0.25)
264	16.38 (±0.46)	14.47 (± 9.42)	4.45 (±0.55)
339	11.58 (±0.04)	5.89 (± 0.79)	5.36 (±0.13)
415	11.58 (±0.03)	4.90 (± 0.39)	5.34 (±0.12)
all data[c]	11.74 (±0.14)	11.29 (± 3.09)	5.11 (±0.22)
	BROMIDE		
36	15.38 (±0.85)	30.94 (±12.23)	6.09 (±0.17)
113[d]	12.57 (-)	0.0 (-)	5.96 (-)
264	16.83 (±0.20)	8.05 (± 3.38)	5.09 (±0.25)
339	11.66 (±0.03)	3.98 (± 0.41)	5.72 (±0.09)
415	11.71 (±0.02)	4.09 (± 0.33)	5.90 (±0.09)
all data[e]	11.66 (±0.10)	5.92 (± 1.91)	5.39 (±0.20)

[a]Values in parentheses represent 95% confidence limits for parameter estimates.

[b]Teflon cup data; all others hollow fiber samplers.

[c]Simultaneous fit to all data except the 188-cm Teflon cup data and the 64-cm depth data.

[d]Best estimates; optimization program failed to converge.

[e]Simultaneous fit to all bromide data, except those of the 264-cm depth.

effective tracer velocity of about 65 cm/d is needed between 188 and 264 cm to give an average v of 14.6 between 0 and 264 cm. This value of 65 cm/day is unrealistically high. Therefore, it seems more likely that the pore water velocity varies significantly horizontally across the caisson and that the 264-cm depth sampler is located in a section of markedly higher hydraulic flux. All of the samplers except the 188- and 264-cm depth hollow fiber units were placed in the left hemisphere of the caisson. Since neither the Teflon sampler in the left hemisphere at the 188-cm depth nor the hollow fiber sampler in the right hemisphere at 188-cm exhibit the apparent high velocity of the 264-cm depth sampler, it must be concluded that the flow path for the fast zone is rather tortuous and not strictly vertical.

The anomalous behavior of the 264-cm depth data may be further elucidated by investigating the behavior of the effluent breakthrough curves for leachate collected from the column exit. Only iodide was measured with sufficient frequency in the effluent to warrant analysis. Observed iodide effluent concentration data are shown in Figure 5. Inspection of these data indicates two distinct peaks suggesting zones in the porous medium moving at two distinctly different velocities. To analyze the data we make the simple and expedient assumption that two flow regions exist which interact negligibly so that the observed effluent concentration C_e is given by

$$C_e = \frac{\sum_{i=1}^{2} A_i q_i c_i}{\sum_{i=1}^{2} A_i q_i} \qquad (14a)$$

$$= \frac{\sum_{i=1}^{2} A_{ri} v_i c_i}{\sum_{i=1}^{2} A_{ri} v_i} \qquad (14b)$$

where A_i is the proportional area of region i with hydraulic flux density q_i from which the local exit concentration is c_i, v_i is the pore water velocity in region i, and $A_{ri} = A_i\,\theta_i$ is the effective hydraulic area where θ_i is the water content in region i. We take $c_i = c_i(x,t;v_i,D_i,t_o,C_i,C_o)$, fix C_i and C_o at their previous values, and estimate v_i, D_i and A_{ri} (i=1,2) and t_o by nonlinear regression analysis of the observed effluent data against (14) with c_i computed via (10). An effective column length of 570 cm was employed assuming the tuff and underlying 25-cm thick sand layer to

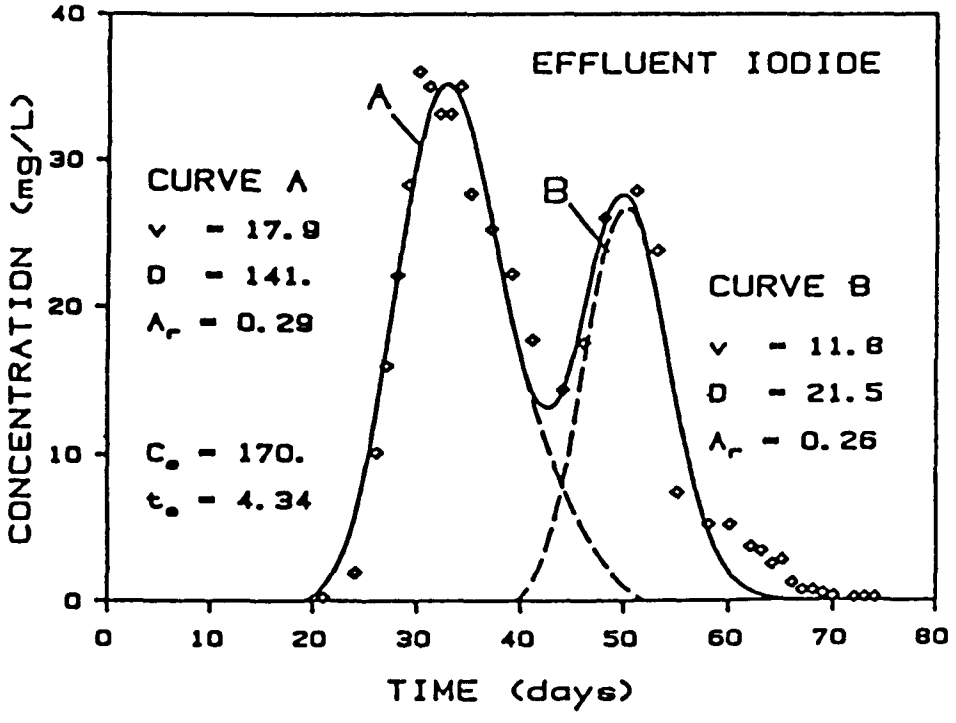

Figure 5. Observed iodide concentrations in effluent from caisson B and fitted curves, assuming two distinct and noninteracting flow regions with different pore water velocities and cross-sectional areas.

have similar properties and the resident time in the lower gravel layer to be insignificant. The results are given in Figure 5. The two apparent flow regions are found to have velocities of 17.9 and 11.8 cm/d corresponding very closely to velocities observed in suction samplers at the 264-cm depth and at the other depths, respectively. The results indicate the effective hydraulic cross-sectional areas of the two regions are nearly equal (A_r=0.29 for the fast zone and 0.26 for the slower zone). In order to elucidate the mechanisms underlying this heterogeneity in the flow field, more detailed spatial resolution of concentrations, water contents, and hydraulic fluxes would be needed.

A simultaneous fit of v, D, and t_o to suction sampler data from all depths, excluding that from the anomalous 264-cm depth and from the 188-cm Teflon sampler (all other data were obtained with hollow fiber samplers), was carried out for iodide and bromide and results are summarized in Table 3. Note that the fitted velocities for iodide and bromide are very similar. Thus, we conclude that the average pore water velocity of 11.7 cm/d estimated from the iodide and bromide tracers is representative of the hydraulic conditions experienced by the majority of the samplers and that this value should be applicable also for the lithium and strontium experiments. As expected, the simultaneously fitted D-values for iodide and bromide are somewhat higher than those for the individual depths because of small differences in local v-values. We also note that the fitted D-values in Table 3 do not indicate any increases with depth due to scale effects. The reverse effect is in fact observed, with D generally decreasing with depth reflecting, as previously suggested, the gradual amelioration in point-source application effects at greater distances. Dispersion coefficients for the iodide effluent data, however, are

considerably higher than for the suction sampler data even without the high flow zone. This is not an unexpected result, since the effluent data reflects heterogenieties over the caisson cross section, whereas suction samples provide a rather localized perspective on the medium.

Using the measured hydraulic flux density of 4.0 cm/d from caisson outflow rate measurements and the estimated average pore water velocity of 11.7 cm/d fitted to the pooled suction sampler data (Tables 3 and 4), we may estimate the effective water content of caisson B during the tracer experiments to be 0.34 cm^3/cm^3. This is greater than the water content measured in the caisson by neutron backscatter, which averaged about 0.28 cm^3/cm^3. If we estimate the mean pore water velocity for the caisson from the iodide effluent data (Figure 5), an area-weighted average of 15 cm/d is obtained corresponding to a water content of 0.27 cm^3/cm^3 which is clearly in better agreement with the observed water contents and thus gives further credence to the postulation of a bimodal velocity distribution.

Observed lithium concentration data for each depth are shown in Figure 6. Individual depth-fitted as well as pooled depth-fitted parameter values of the estimated parameters R, D, and t_o are given in Table 4. Note that the pooled depth-fitted R is 1.18, indicating a small amount of lithium adsorption.

Inspection of the data in Tables 3 and 4 reveals relatively large differences in D for the different ports. In part this may be due to somewhat poor identifiability of D, as evidenced by the relatively wide 95% confidence intervals, especially for the lithium data. The average of the D-values of iodide and bromide at 339- and 415-cm depths is 4.72 cm^2/d. This value is well within the 95% confidence range for the lithium data.

Because D-values at greater depths also partially reflect transport properties of the soil medium closer to the soil surface, we chose to fix D at the above-average value of 4.72 cm^2/d independently of depth or tracer to simulate all suction sampler data. Given this estimate for D, the previously estimated value for v of 11.7 cm/d, and a mean value for t_o of 5.43 d derived from all fitted pulse times in Tables 3 and 4, the sampler breakthrough curves for iodide, bromide, and lithium can be calculated.

Table 4. Estimated values for the dispersion coefficient D, the retardation factor R, and the pulse time t_o for the lithium experiments in caisson B assuming v=11.7 cm/d.

Depth (cm)	D (cm^2/d)	R (-)	t_o (d)
36	27.50 (±24.34)	0.789 (±0.102)	6.42 (±0.41)
113	10.57 (±5.73)	1.133 (±0.039)	5.46 (±0.55)
188	9.96 (±3.52)	1.138 (±0.024)	5.44 (±0.52)
188[a]	5.96 (±3.11)	1.070 (±0.025)	5.33 (±0.50)
264[b]	14.80 (±5.18)	0.844 (±0.018)	5.24 (±0.59)
264[c]	20.99 (±7.35)	1.197 (±0.026)	5.24 (±0.59)
415	8.69 (±5.40)	1.227 (±0.025)	4.89 (±1.04)
all data[d]	12.58 (±5.43)	1.180 (±0.027)	5.25 (±0.42)

a Teflon cup data.

b Assuming v=11.7 cm/d.

c Assuming v=16.6 cm/d.

d Simultaneous fit to all observations except the 188-cm teflon cup data and the 264-cm-depth data.

Results are shown as the solid lines Figures 3, 4, and 6. The observed data are fairly well described at all depths except at 264 cm where the previously noted fast flow zone was observed.

To predict strontium transport, we employed the values for v and D estimated from the pooled iodide, bromide, and lithium data and independently estimated values of all other parameters except the Freundlich coefficients k. The last of these was estimated from the initial breakthrough part of the 188-cm hollow fiber sampling data to be 1.486 in units consistent with those of c (mg/L) and s(mg/g). Observed and calculated breakthrough curves for all depths are shown in Figure 7. The observed data, especially the peak concentrations, at different depths are extremely erratic and inconsistent. Despite these inconsistencies, the assumed parameters lead to surprisingly accurate predictions of initial breakthrough at most depths, except again for the 264-cm port. Peak concentrations are accurately described in only one or two cases (at 188 and 339 cm), with severe deviations occurring at the 36-, 113- and 264-cm depth ports. Poor apparent mass balance is obtained at several depths.

The exact reasons for this behavior are not clear. Strontium adsorption on the samplers might be suggested as an explanation, except that two of the hollow fiber samplers do show reasonable mass balances. Another explanation could be that local compaction of soil around the samplers results in stagnant liquid zones in which transport is controlled largely by diffusion. While immobile water zones can have marked effects on transport of strongly adsorbed tracers (van Genuchten 1985), we tend to discount mobile-immobile effects in this case for two reasons. First, there is not evidence of similar behavior for the iodide, bromide, and

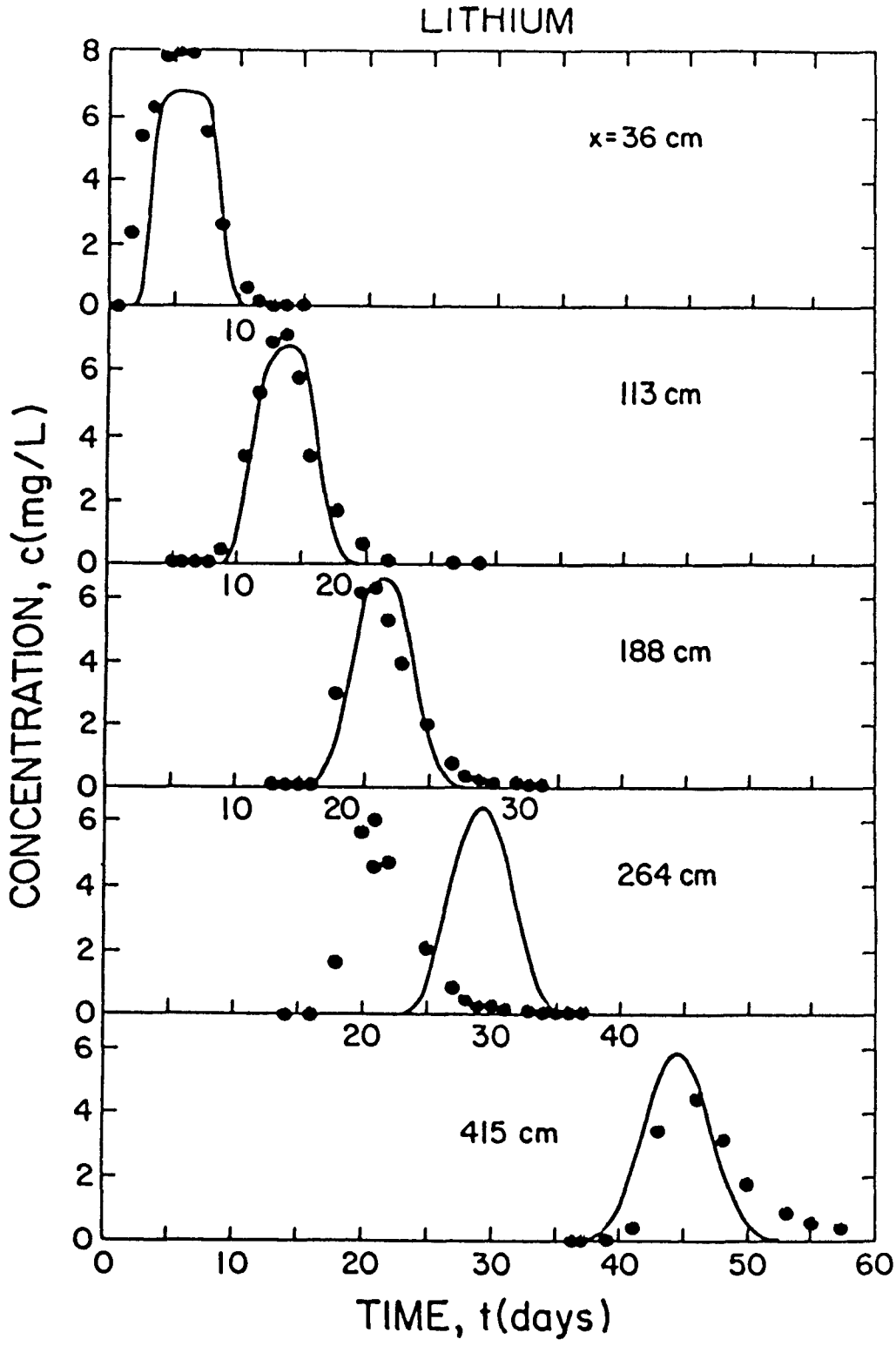

Figure 6. Lithium breakthrough curves measured at various depths in hollow fiber samplers and predicted curves using parameter values estimated from pooled iodide, bromide, and lithium data.

lithium tracer data. Minor tailing in the lithium breakthrough curves could have been caused by immobile water but also by some nonlinear adsorption effects (data are insufficient to draw definite conclusions). Second, if immobile zones were present, the observed breakthrough curves should have been displaced to the right of those in Figure 7 because of the slow diffusional processes. This is clearly not the case as the initial breakthrough at all depths (except at 264 cm) are reasonably well described.

A more probable explanation for the observed behavior of strontium is that the precipitation of $SrCO_3$, either <u>in situ</u> or in the solution samples after extraction from the caisson has occurred, results in apparent erratic mass balance. This explanation seems especially probable because of the high pH (approximately 8) and low temperatures (approximately 5^oC) in the caisson during the experiment, which would favor the stability of $SrCO_3$. Furthermore, the fact that the tuff was crushed may have increased the potential for weathering and the possible release of additional alkalinity into the soil solution. Tentative calculations based on measured chemical data suggest that the soil solution may have been supersaturated with respect to $SrCO_3$. Degassing of the extracted soil solution during sampling may have promoted even higher pH-values and thus further increased the likelihood of $SrCO_3$ precipitation (Suarez 1986a), which could lead to erratic apparent solution concentrations. The use of extractors that limit or prevent degassing (Suarez 1986b) should be considered in similar studies that may be conducted in the future if strontium is employed as a tracer.

From the fitted k-value of 1.486 and the estimated η-value of 0.835 (Polzer et al. 1985), we obtain the following Freundlich isotherm for strontium adsorption on Bandelier Tuff:

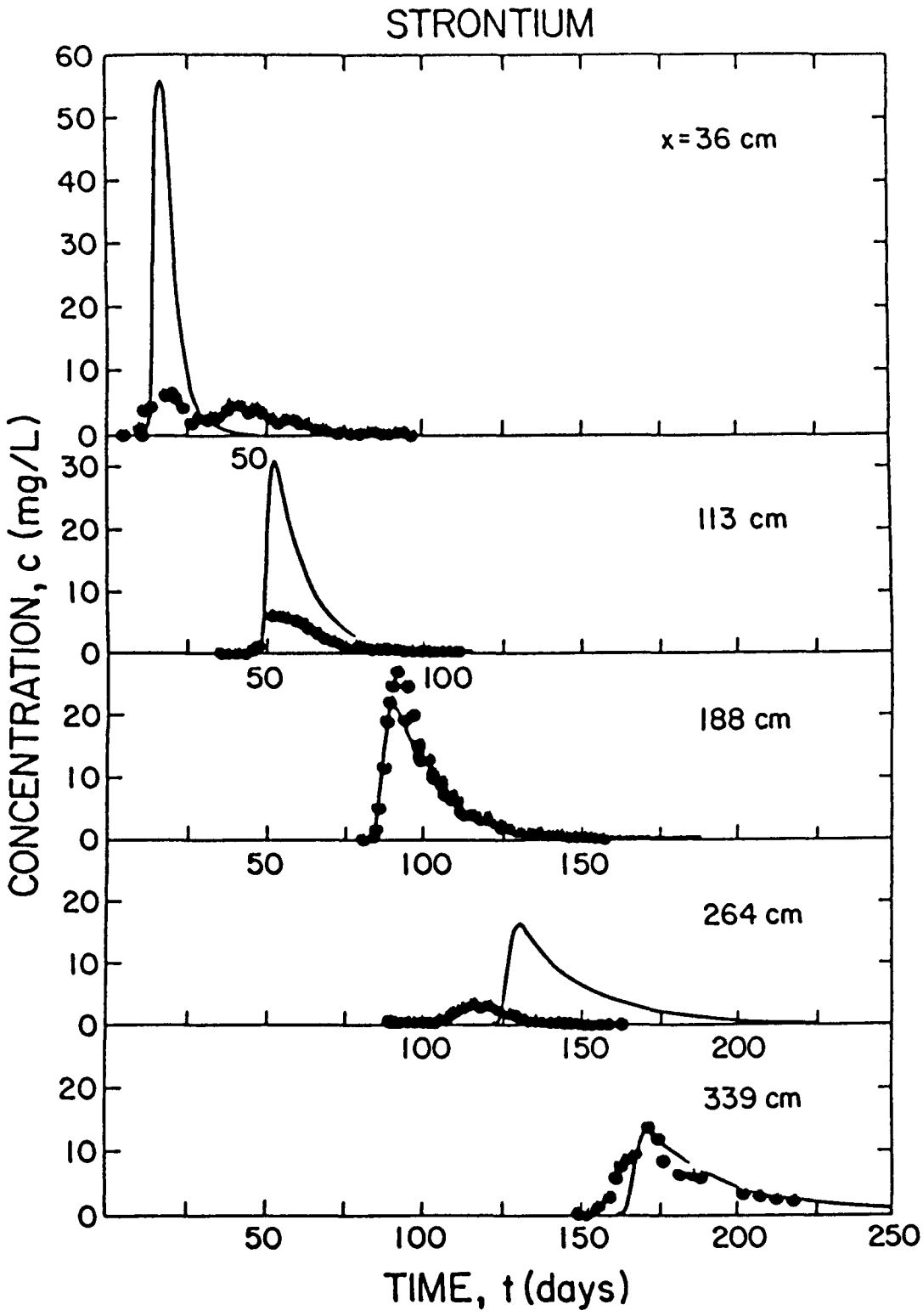

Figure 7. Strontium breakthrough curves measured at various depths in hollow fiber samplers and predicted curves using estimated parameter values.

$$s = 1.486\ C^{0.835}. \qquad (15)$$

This equation can be linearized in several ways. One way is to assume that the areas under the linearized isotherm ($s=k_dC$) and the nonlinear isotherm are the same for the range in concentration values used in the displacement experiment (van Genuchten 1981):

$$\int_0^{c_a} k_dC\ dC = \int_0^{c_a} 1.486\ C^{0.835} dC\ . \qquad (16)$$

Assuming an average peak concentration c_a of 50 mg/L during the leaching experiment results in a k_d value [Equation (16)] of 0.85 g/mL corresponding to a retardation factor R of about 5.85. When substituted into Equation (10), this R-value leads to reasonable predictions of the locations of the peak concentration in the caisson (results not shown here). The strontium peak concentration at the 188-cm port was actually predicted somewhat better than with the more rigorous nonlinear model. However, the asymmetrical shape of the observed breakthrough curves will not be described well by the linear model, which produces relatively symmetric curves for the magnitude of hydrodynamic dispersion in these experiments. The value of K_d estimated in the above manner from the caisson tracer experiments is observed to be much higher than that estimated by Polzer et al. (1985) from batch equilibrium studies. Occurrence of $SrCO_3$ precipitation in the caisson experiments may explain the high apparent distribution coefficient for Sr. At the higher temperatures and much lower solid-solution ratios of the laboratory batch studies, the stability of $SrCO_3$ may be anticipated to be much lower than in these field studies.

SUMMARY AND RECOMMENDATIONS

In this study we have investigated the use of various simple deterministic models to describe flow and transport behavior of crushed Bandelier Tuff in large lysimeters. Parameter estimation methods have been found to facilitate accurate model calibration. In many respects, the simple flow and transport models have provided quite adequate description of the observed behavior. However, it is evident that even in this fabricated and presumably rather homogeneous medium, considerable variability in flow and transport behavior occurs that complicates the description and prediction of these processes. A number of specific observations and suggestions for subsequent studies follow:

1. The hydraulic properties of Bandelier Tuff appear to be well characterized by the assumed parametric model. The model provides reasonable predictions of transient unsaturated flow behavior except when very near to saturation.

2. Considerable ambiguity occurred in the interpretation of influent concentrations and pulse durations, which had to be adjusted rather arbitrarily to obtain apparent mass balances even for presumably nonreactive tracers. In future experiments greater precision in characterizing the input function should be sought by making more frequent measurements of influent concentrations, feed rates, and pulse durations.

3. A few additional concentration measurements during the time interval in which the pulses pass given depths would allow for a better definition of v, t_o, and especially D for species with little or no retardation (iodide, bromide, and lithium).

4. More detailed geochemical analyses should be performed to investigate the possibility of $SrCO_3$ precipitation in these or similar experiments.

There are indications that the soil solution was supersaturated with respect to $SrCO_3$ resulting in erratic apparent mass balances for strontium and larger than expected retardation. In order to study this phenomenon experimentally, consideration will need to be given to the use of extractors that limit the degassing of samples.

5. Attention should be addressed to the evaluation of variability in transport behavior. The results indicate that even in this relatively homogeneous, artificially constructed medium, significant variations in water contents and/or hydraulic fluxes occur within the caissons. Multiple sampling ports should be placed at each depth to evaluate the structure of the heterogeneity and isolate its cause; to conserve effort, it may be satisfactory to reduce the number of depths sampled while increasing the number of ports per depth.

6. The water/tracer application system should be redesigned to obtain a more uniform addition of solution at the caisson surface. This would better simulate natural conditions and eliminate the apparent high dispersion at shallow depths. Uneven distribution may also contribute to transverse velocity variations by encouraging local fingering of the flow paths.

7. In order to preclude any uncertainty in measured water contents in future studies, it may be advisable to obtain a few gravimetric samples to check the neutron probe calibration.

REFERENCES

Abeele, W. V. 1979. Determination of hydraulic conductivity in crushed Bandelier Tuff. Los Alamos National Laboratory report LA-8147-MS.

Abeele, W. V. 1984. Hydraulic testing of crushed Bandelier Tuff. Los Alamos National Laboratory report LA-10037-MS. 21 p.

DePoorter, G. L. 1981. The Los Alamos experimental engineered waste burial facility: Design considerations and preliminary experimental plan. In: Waste Management '81. R. G. Post and M. E. Wacks (eds.), Univ. Arizona. pp. 667-686.

Kool, J. B., J. C. Parker, and M. Th. van Genuchten. 1985. ONESTEP: A nonlinear parameter estimation program for evaluating soil hydraulic properties from one-step outflow measurements. Virginia Agric. Exp. Sta. Bull. 85-3. 43 pp.

Marquardt, D. W. 1963. An algorithm for least-squares estimation of nonlinear parameters. SIAM J. Appl. Math. 11:431-441.

Mualem, Y. 1976. A new model for predicting the hydraulic conductivity of unsaturated porous media. Water Resour. Res. 12:513-522.

Parker, J. C., and M. Th. van Genuchten. 1984a. Flux-averaged and volume-averaged concentrations in continuum approaches to solute transport. Water Resour. Res. 20:866-872.

Parker, J. C., and M. Th. van Genuchten. 1984b. Determining transport parameters from laboratory and field tracer experiments. Bulletin 84-3, Virginia Agric. Exp., Blacksburg, Virginia. 96 pp.

Parker J. C., J. B. Kool, and M. Th. van Genuchten. 1985. Determining soil hydraulic properties from one-step outflow experiments by parameter estimation, II. Experimental studies. Soil Sci. Soc. Am. J. 49:1354-1359.

Polzer, W. L., H. R. Fuentes, E. H. Essington, and F. Roensch. 1985. Equilibrium sorption of cobalt, cesium and strontium on Bandelier Tuff: Analysis of alternative mathematical modeling. In R. G. Post (ed.), Waste Management '85, Proc. of the Symposium on Waste Management, Tucson, Arizona (March 24-28, 1985). Vol. 3, pp. 167-173.

Suarez, D. L. 1986a. Prediction of pH errors in soil water extractors due to degassing. Soil Sci. Soc. Am. J. (submitted).

Suarez, D. L. 1986b. A soil water extractor that minimized CO_2 degassing and pH errors. Water Resour. Res. (in press).

van Genuchten, M. Th. 1980. A closed-form equation for predicting the hydraulic conductivity of unsaturated soils. Soil Sci. Soc. Am. J. 44:892-898.

van Genuchten, M. Th. 1981. Non-equilibrium transport parameters from miscible displacement experiments. Research Report 119, U. S. Salinity Laboratory, USDA-SEA, Riverside, California. 88 pp.

van Genuchten, M. Th. 1985. Solute transport in structured soils. In: H. J. Morel Seytoux (eds.), Proc. 5th Annual AGU Front Range Branch Hydrology Days, Hydrology Days Publ., Ft. Collins, Colorado. 169-180 pp.